

... ..

...

S a e Ke Lab a | C e Ne ce ce a d
Lea , Be N a U e | , Be , Ç a



...

S a e Ke Lab a | C e Ne ce ce a d
Lea , Be N a U e | , Be , Ç a



...

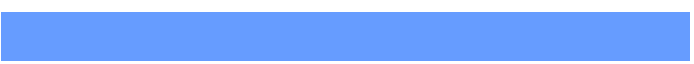
S a e Ke Lab a | C e Ne ce ce a d
Lea , Be N a U e | , Be , Ç a



De a e P | , Pe -T r a Ce e
L e S ce ce , a d PKU-IDG/McG e l e B a
Re ea ç , Pe U e | , Be , Ç a



...



suppressed the untrained retinal locations (J. Y. Zhang et al., 2010), as hinted by the known neurophysiological impacts of spatial attention inhibiting unattended regions (Moran & Desimone, 1985; Treue, 2001; Slotnick, Schwarzbach, & Yantis, 2003), even if these regions are unstimulated (Smith, Singh, & Greenlee, 2000; Shmuel, Augath, Oeltermann, & Logothetis, 2006), as is typical in perceptual learning studies.

In addition, location-specific learning may transfer to a mirrored location in the opposite hemisphere when the training and transfer



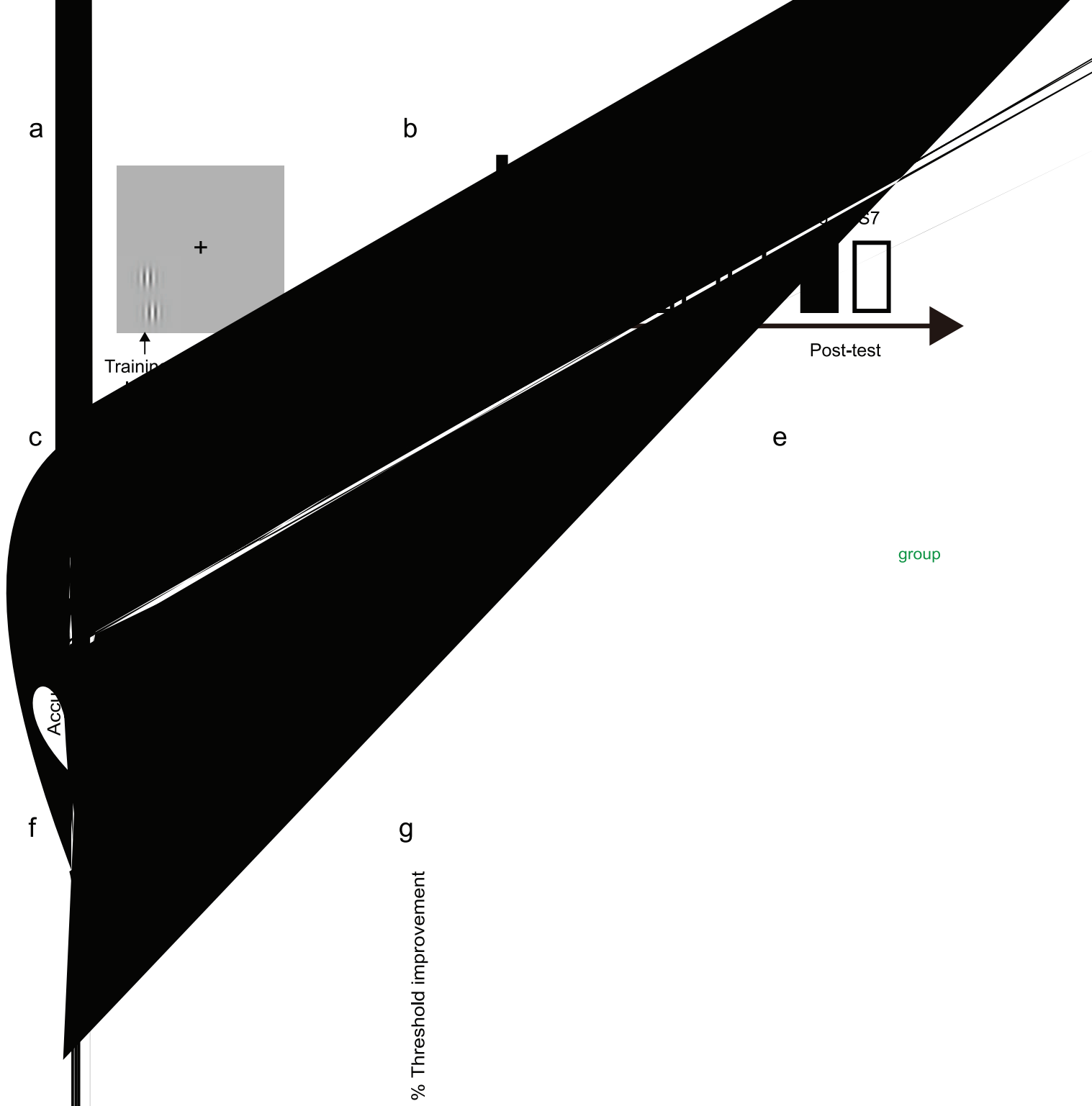
Vernier alignment thresholds were measured with a single-interval 2AFC staircase procedure. In each trial, the stimulus was presented for 200 ms. The observer's task was to judge whether the upper Gabor was to the left or right of the lower Gabor. A small foveal fixation cross ($25' \times 25'$) preceded each trial by 500 ms and stayed throughout the trial. Auditory feedback was given on incorrect responses in behavioral sessions, but not in ERP sessions. The staircase followed a 3-down-1-up rule, which resulted in a 79.4% convergence rate (Levitt, 1971). The step size of the staircase was 0.05 log units. The geometric mean of the reversals, excluding the first five, was taken as the threshold. Each staircase consisted of 125 trials in training sessions but in a pretraining baseline session, these trials also interleaved with another 125 trials with a fixed subthreshold Vernier offset (see Results). There was a brief rest every 42 trials to reduce fatigue.

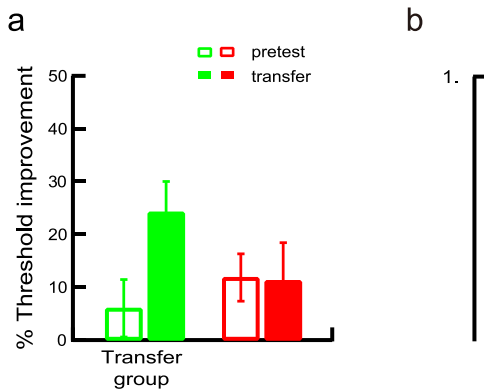
The electroencephalogram (EEG) was recorded by a NeuroScan system (Neurosoft, Inc., Sterling, VA, USA) with 64 silver chloride electrodes mounted on an elastic cap according to the international 10-20 system. The electrode activity of the brain was amplified and digitized continuously (bandpass filtered at 0.05–100 Hz) at a sample rate of 1000 Hz. The horizontal electrooculogram (EOG) was recorded from two electrodes positioned at the outer canthus of each eye, and the vertical EOG was recorded from two electrodes located below and above the left eye. All electrodes, except those for monitoring eye movements, were physically referenced to the left mastoid and were then off-line re-referenced to the average of the left and right mastoids. Electrode impedances were kept below 5 k Ω .

The experiment consisted of eight sessions in seven different days (Figure 2b): A practice session (S0) and an ERP baseline session (S1) on the first day, four behavioral training sessions (S2–S5), an ERP posttraining session (S6), and a behavioral posttraining session (S7). In the practice session (S0), each observer practiced 40 trials in a staircase at the to-be-trained location to get familiar with the task. The baseline session (S1) consisted of four 250-trial blocks, in which the EEG signals were recorded. Half the trials in each block were controlled by a staircase procedure to converge the Vernier offset to the threshold level (mean

Vernier offset 4.53 ± 0.26 arcmin). The other half remained at a fixed subthreshold level based on practice performance (mean Vernier offset 2.88 ± 0.08 arcmin). To determine these subthreshold offset values, the Vernier offset was first set 3 arcmin, close to the mean posttraining threshold of a separate group of eight observers who in a prep experiment performed the same near-threshold Vernier training without ERP recording. This measure would not only approximately determine the mean Vernier offset subthreshold, but also allow near-threshold ERP comparisons before and after training (Figure 7). Then this 3-arcmin subthreshold offset was compared to a very rough estimate of the threshold offset in S0 (the mean of the last 25 trials) for each observer. Depending on the difference between these two offsets, the final subthreshold offset was adjusted individually by 0, ± 0.5 , or ± 1 arcmin for most observers (with a few exceptions in which the adjustment did not use the exact 0.5-arcmin steps, see Figure 3c). These two types of trials were randomly interleaved trial by trial. Each training session (S2–S5) included eight 125-trial staircases. The ERP posttraining session (S6) included four 250-trial blocks. The Vernier offset in half the trials of each block was fixed at the pretraining threshold level, and in the other half was at the pretraining subthreshold baseline level. These trials were also randomly interleaved trial by trial. The behavioral posttraining session (S7) consisted of four 125-trial staircases, two at the trained location and two at the untrained location in a counterbalanced order. Vernier training was always performed in the lower-left visual quadrant (S2–S5), and the pre- and posttraining behavioral and ERP performance were measured in both the trained lower-left and untrained lower-right visual quadrants, each quadrant with half of the trials (S1, S6, and S7).

The amount of perceptual learning was quantified by the accuracy improvement from S1 to S6 and by the percent threshold improvement from S1 to S7. The amount of learning transfer was quantified by the transfer index (TI) that was calculated as the accuracy improvement at the untrained location divided by the accuracy improvement at the trained location, so that $TI \geq 1$ indicated complete transfer and $TI \leq 0$ indicated no transfer. Here we used accuracy changes to calculate TIs because the accuracies were measured during ERP recording, so that the relationship between TIs and ERP changes could be directly examined.





Raw EEG data were first off-line filtered with a digital band-pass of 0.1–40 Hz. Each epoch of EEG ranged from 200 ms before stimulus onset to 800 ms after stimulus onset. Baseline was corrected by subtracting the mean of the signals within the time window of -200 ms to 0 ms (stimulus onset). Trials with eye blinks, eye movements, muscle potentials exceeding ± 50 μ V at any electrode, or with incorrect behavioral responses, were excluded from ERP averaging. The numbers of trials were matched between ERP baseline sessions and ERP posttraining sessions by randomly selecting epochs from sessions containing more trials in each observer. There were about 150 stimulus-related EEG epochs averaged for each condition.

Six posterior electrodes in each hemisphere (P1, P3, P5, PO3, PO5, and PO7 in the left hemisphere and P2, P4, P6, PO4, PO6, and PO8 in the right hemisphere), which covered the posterior cortex with the most visible P1-N1 changes (Figure 4), were selected for statistical analysis. For each observer, we averaged signals from six electrodes at each hemisphere to increase the signal-to-noise ratio. Paired two-tailed t -tests were applied to test ERP differences between pre- and posttraining conditions in each of the 5-ms bins. Most comparisons were performed within a time window between 120 and 200 ms, with an exception for waveforms evoked by stimuli presented at the untrained location with the “specificity” group (see Results), under which a time window between 165 and 200 ms was selected (the pre- and posttraining ERPs between 120 and 165 ms had no visible differences). Multiple comparisons with respect to the number of bins were corrected using the Benjamini-Hochberg (1995) false discovery rate (FDR) correction with $\alpha = 0.05$.

The accuracy of discriminating the Vernier offset in the trained lower-left visual quadrant was improved significantly by $7.2\% \pm 1.0\%$ (averaged over both Vernier offset conditions, $p < 0.001$, one-tailed paired test; Figure 2c) from S1 to S6. The accuracy in the untrained lower-right quadrant was also improved by $2.9\% \pm 1.0\%$ ($p = 0.004$) over the same period, indicating overall partial transfer of Vernier learning (TI $= 0.41 \pm 0.10$). However, the amount of learning transfer varied greatly among observers, as can be appreciated by the individual accuracy improvement at the transfer location plotted against the accuracy improvement at the trained location (Figure 2d), as well as by individual TI variations (Figure 2e). We divided the observers into a “transfer” group ($n = 15$; TI > 0.5) and a “specificity” group ($n = 13$; TI < 0.5), which allowed later transfer versus specificity comparisons of ERP changes. The mean Vernier accuracy at the untrained locations was improved by $7.0\% \pm 0.7\%$ ($p < 0.001$) in the “transfer” group (TI $= 0.84 \pm 0.05$) and $1.1\% \pm 1.1\%$ ($p = 0.16$) in the “specificity” group (TI $= 0.03 \pm 0.08$; Figure 2c). These results were confirmed by significant threshold decreases ($24.2\% \pm 5.8\%$, $p < 0.001$) in the “transfer” group and insignificant threshold changes ($11.3\% \pm 7.3\%$, $p = 0.07$) in the “specificity” group at the untrained location from S1 to S7 (Figure 2f and g). Here the “transfer” and “specificity” groups had similar pre-training accuracies with subthreshold Vernier stimuli ($71.4\% \pm 1.3\%$ vs. $69.6\% \pm 1.3\%$, $p = 0.34$, two-tailed Student’s t -test; the theoretical accuracies at threshold were identical at 79.4%) and pretraining thresholds (4.3



± 0.4 arcmin vs. 4.8 ± 0.3 arcmin, $r = 0.28$, Figure 2f), as well as accuracy improvements ($7.6\% \pm 1.1\%$ vs. $6.8\% \pm 1.7\%$, $r = 0.67$, Figure 2c) and threshold improvements ($32.9\% \pm 3.3\%$ vs. $33.8\% \pm 3.5\%$, $r = 0.85$, Figure 2g) after training, all at the trained location. Therefore the observers in two groups were homogeneous in these dimensions.

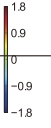
It was unlikely that the transfer of Vernier learning in the “transfer” group was a result of the S1 pretest at the untrained location. We calculated the average Vernier threshold improvement from S1 to the mean of the first four staircases (half of the total staircases) in S2 at the trained location in the “transfer” group to estimate the impact of pretest at the untrained location, which was very small ($6.0\% \pm 5.4\%$, $r = 0.15$), about a quarter of the 24.2% overall threshold improvement at the untrained location (Figure 3a). For the “specificity” group, the corresponding S1 pretest effect was $11.8\% \pm 4.5\%$ ($r = 0.01$), similar to the 11.3% threshold improvement at the untrained location. In addition, the slopes of the simple regression lines of the transfer index versus the pretest impact functions were insignificantly different from zero in both the “transfer” groups (slope 0.0045 , $r = 0.064$) and the “specificity” group (slope 0.0032 , $r = 0.46$) (Figure 3b), indicating that how much Vernier learning transfers was not significantly affected by pretests in this experiment. The transfer of Vernier learning was also not affected by initial group differences of Vernier offsets, as the initial Vernier offsets did not differ between the “transfer” group and “specificity” group at the threshold ($r = 0.28$) and subthreshold levels ($r = 0.47$) (Figure 3c).

ERP was recorded under two Vernier offset conditions pre- and posttraining in S1 and S6: The “subthreshold pre” condition and the “threshold pre” condition. Under the “subthreshold pre” condition, the Vernier offsets fixed at the pretraining subthreshold levels changed to near-threshold after training at the trained location (mean offset 2.88 ± 0.08 arcmin, which was lower than the mean pretraining threshold 4.53 ± 0.26 arcmin and near the mean post-training threshold 3.10 ± 0.19 arcmin in S7). Under the “threshold pre” condition, the pretraining Vernier offsets were not fixed but varied around the thresholds under the control of the staircases. Although this

measure would increase the noise of ERP responses (the first 30 trials of each staircase were thrown out to reduce the Vernier offset variation to $SD = 0.34$ arcmin), the more problematic practice effect was avoided if behavioral pretraining thresholds were measured before ERP pretraining baselines. The post-training Vernier offsets were fixed at the pretraining threshold levels. Therefore, under the “threshold pre” condition the Vernier offsets changed from threshold levels to suprathreshold levels after training at the trained location.

The mean topographic maps and ERP waveforms are presented in Figure 4 for the “subthreshold pre” condition and Figure 5 for the “threshold pre” condition. The first visual ERP component C1 could not be reliably identified and analyzed, likely due to the small stimulus size and low stimulus contrast, as well as the possibility that some observers may not show significant C1 responses to the stimulus presented at this specific location (Kelly, Gomez-Ramirez, & Foxe, 2008). Two issues are worth noting before detailed analysis of the impacts of learning and its specificity/transfer on ERP responses. First, the pretraining ERP waveforms were not significantly different between the two groups ($p > 0.05$ after FDR correction) in the ipsilateral and contralateral posterior cortices under the “subthreshold pre” and “threshold pre” conditions, respectively, within a time window of 120–200 ms (covering P1 and N1, see below). Therefore, learning transfer/specificity was unrelated to neither the pretraining thresholds (Figure 2f) nor the pretraining ERPs. Second, when the Vernier task under the “threshold pre” condition was performed at the untrained location (Figure 5), the peaks of difference waveforms (posttraining – pretraining) of the “transfer” group were significantly different from those of the “specificity” groups within the 120–200 ms time window. ($F(1, 26) = 12.8$, $p = 0.001$, mean amplitudes of 10-ms time windows around the peak over six selected electrodes in each hemisphere were entered into a repeated measures ANOVA. We did not run t tests here because the latencies of peaks were different between the “transfer” and “specificity” groups, see green lines in Figures 4 and 5.) These differences indicated that the observers could be reliably divided into “transfer” and “specificity” groups on the basis of not only behavioral improvements, but also ERP changes.

Some interesting patterns of ERP changes, which were similar under “subthreshold pre” and “threshold pre” Vernier offset conditions, emerged that were



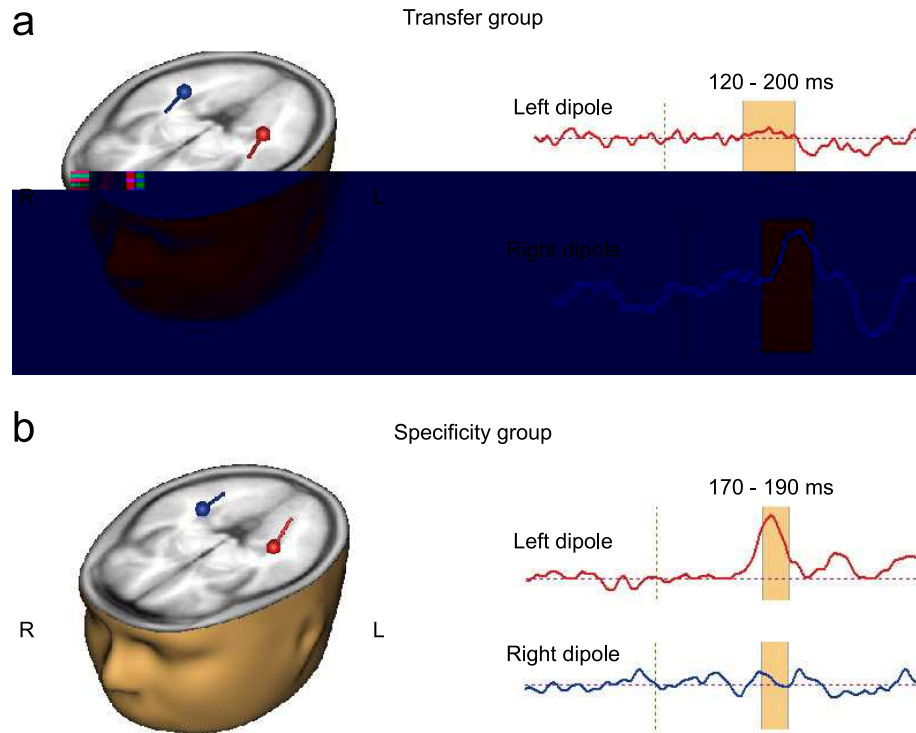


Figure 6. Source localization of ERP for the Vernier task. (a) and (b) show the “transfer” and “specificity” groups, respectively. The topographic maps show the location of the dipoles. The waveforms show the ERP changes in the ipsilateral posterior cortex (120–200 ms) and the contralateral posterior cortex (170–190 ms). The shaded areas indicate the significant changes in the ERP.

distinctly associated with the “transfer” and “specificity” groups, respectively. Under the “subthreshold pre” condition (Figure 4), the Vernier task performed by the “transfer” group at the trained lower-left visual quadrant evoked reduced P1 and enhanced N1 in the ipsilateral posterior cortex (145–200 ms), although there were no significant ERP changes in the contralateral posterior cortex. The same task performed at the untrained lower-right visual quadrant also revealed reduced P1 and enhanced N1 (120–200 ms) in the ipsilateral hemisphere, as well as reduced contralateral P1 (130–150 ms). The patterns of these P1-N1 changes due to training and transfer are thus similar, and at least the ERP changes with the Vernier task at the untrained location should reflect top-down influences. However, ERP changes associated with Vernier task performed by the “specificity” group at the trained location were weaker and more limited, and those at the untrained location were very different or even opposite. When the Vernier task was performed at the trained location, only P1 in the ipsilateral posterior

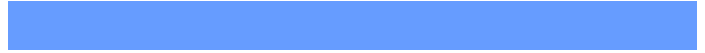
cortex (140–160 ms) was reduced. There was no significant N1 change, in contrast to widespread N1 enhancement in the “transfer” group. When the Vernier task was performed at the untrained location, no P1 reduction and N1 enhancement were observed, in contrast to significant P1 reduction and N1 enhancement in the “transfer” group. In addition, N1 in the contralateral posterior cortex (170–190 ms) was suppressed.

Similar patterns of ERP changes were observed under the “threshold pre” condition (Figure 5). For the “transfer” group the Vernier task at the trained location evoked smaller P1 and larger N1 responses in the ipsilateral posterior cortex (145–190 ms) and the contralateral posterior cortex (130–175 ms). The same task at the untrained location also evoked smaller P1 and larger N1 responses in the ipsilateral posterior cortex (140–200 ms), as well as larger contralateral N1 in a narrow time window (160–175 ms). For the “specificity” group the Vernier task at the trained location evoked larger ipsilateral N1 responses only in

Figure 4. Source localization of ERP for the Vernier task. (a) and (b) show the “transfer” and “specificity” groups, respectively. The topographic maps show the location of the dipoles. The waveforms show the ERP changes in the ipsilateral posterior cortex (145–200 ms) and the contralateral posterior cortex (170–190 ms). The shaded areas indicate the significant changes in the ERP.

hemisphere and P2, P4, P6, PO4, PO6, and PO8 in the right hemisphere). A significant Group \times Hemisphere interaction, ($F(1, 26) = 5.97, p = 0.022$), confirmed the source difference between the P1 reduction and N1 enhancement with the “transfer” group and the N1 suppression with the “specificity” group.

In Figures 4 and 5 the ERP P1-N1 changes were estimated on the basis of pre- and posttraining ERP waveforms associated with the same physical Vernier offsets. However, at least under the “threshold pre” condition, the Vernier offsets changed from near-threshold to suprathreshold, so that the task difficulty and attention demand were reduced as a result of learning, which could have confounded the explanation of the ERP effects. To clarify this issue, we calculated the differences between pretraining waveforms under the “threshold pre” condition and



connections: When Vernier learning shows location specificity, contralateral N1, which is corresponding to the untrained retinal location when the Vernier task is performed at this location, is inhibited. Moreover, the top-down influences from high-level learning, as evidenced by the P1 reduction and N1 enhancement, are blocked completely when the Vernier task is at the untrained hemisphere, as well as greatly weakened and limited when the Vernier task is at the trained hemisphere (only a small area is trained, so other areas of the same hemisphere are likely suppressed too).

Previous ERP evidence shows that the visual N1 amplitude is larger when attention is directed to a retinal location where stimuli are presented than when directed to other locations (Luck & Hillyard, 1995; Mangun, 1995). However, in our study P1-N1 changes are evident with perceptual learning regardless of whether the post-training Vernier task is near threshold or suprathreshold (Figure 7). These results excluded the possibility that P1-N1 changes result from reduced task difficulty and attention demand as a result of perceptual learning. We speculate that the P1-N1 changes may reflect top-down modulation of high level decision-making as a result of perceptual learning. On the basis of psychophysical learning transfer data, especially those showing transfer across orthogonal orientations (which also excludes perceptual learning being improved attention to a specific feature dimension, e.g., a specific orientation), we suggest that perceptual learning is decision-making learning in that the observers learn the rules of reweighing the sensory inputs through training (Zhang et al., 2010a). This decision-making learning proposal is consistent with recent neurophysiological and fMRI evidence that brain areas responsible for decision making, such as the lateral intraparietal area (LIP) and the anterior cingulate cortex (ACC), are involved in perceptual learning (Law & Gold, 2008; Kahnt, Grueschow, Speck, & Haynes, 2011).

This research was supported by Natural Science Foundation of China Grants 31230030 (CY) and 31070899 (YS).

Commercial relationships: none.

Corresponding author: Cong Yu and Yan Song.
Email: yucong@pku.edu.cn; songyan@bnu.edu.cn.
Address: Department of Psychology and Peking-Tsinghua Center for Life Sciences, Peking University, Beijing, China; State Key Laboratory of Cognitive

Neuroscience and Learning, Beijing Normal University, Beijing, China.

- Bejjanki, V. R., Beck, J. M., Lu, Z. L., & Pouget, A. (2011). Perceptual learning as improved probabilistic inference in early sensory areas. *Journal of Neuroscience*, *31*(15), 642–648.
- Benjamini, Y., & Hochberg, Y. (1995). Controlling the false discovery rate: A practical and powerful approach to multiple testing. *Biometrika*, *82*(1), 289–300.
- Berardi, N., & Fiorentini, A. (1987). Interhemispheric transfer of visual information in humans: Spatial characteristics. *Journal of Experimental Psychology: Applied*, *3*(4), 633–647.
- Crist, R. E., Kapadia, M. K., Westheimer, G., & Gilbert, C. D. (1997). Perceptual learning of spatial localization: Specificity for orientation, position, and context. *Journal of Experimental Psychology: Applied*, *3*(6), 2889–2894.
- Kahnt, T., Grueschow, M., Speck, O., & Haynes, J. D. (2011). Perceptual learning and decision-making in human medial frontal cortex. *Journal of Experimental Psychology: Applied*, *17*(3), 549–559.
- Karni, A., & Sagi, D. (1991). Where practice makes perfect in texture discrimination: Evidence for primary visual cortex plasticity. *Journal of Experimental Psychology: Applied*, *1*(11), 4966–4970.
- Kelly, S. P., Gomez-Ramirez, M., & Foxe, J. J. (2008). Spatial attention modulates initial afferent activity in human primary visual cortex. *Journal of Experimental Psychology: Applied*, *14*(11), 2629–2636.
- Law, C. T., & Gold, J. I. (2008). Neural correlates of perceptual learning in a sensory-motor, but not a sensory, cortical area. *Journal of Experimental Psychology: Applied*, *14*(4), 505–513.
- Levitt, H. (1971). Transformed up-down methods in psychoacoustics. *Journal of Experimental Psychology: Applied*, *1*(2), 467–477.
- Luck, S. J., & Hillyard, S. A. (1995). The role of attention in feature detection and conjunction discrimination: An electrophysiological analysis. *Journal of Experimental Psychology: Applied*, *1*(1-4), 281–297.
- Mangun, G. R. (1995). Neural mechanisms of visual selective attention. *Journal of Experimental Psychology: Applied*, *1*(1), 4–18.
- Moran, J., & Desimone, R. (1985). Selective attention

- gates visual processing in the extrastriate cortex. *Journal of Neuroscience*, (4715), 782–784.
- Pelli, D. G. (1997). The VideoToolbox software for visual psychophysics: Transforming numbers into movies. *Journal of Vision*, (4), 437–442.
- Schoups, A., Vogels, R., & Orban, G. A. (1995). Human perceptual learning in identifying the oblique orientation: Retinotopy, orientation specificity and monocularity. *Journal of Vision*, (Pt 3), 797–810.
- Shmuel, A., Augath, M., Oeltermann, A., & Logothetis, N. K. (2006). Negative functional MRI response correlates with decreases in neuronal activity in monkey visual area V1. *Journal of Vision*, (4), 569–577.
- Slotnick, S. D., Schwarzbach, J., & Yantis, S. (2003). Attentional inhibition of visual processing in human striate and extrastriate cortex. *Journal of Vision*, (4), 1602–1611.
- Smith, A. T., Singh, K. D., & Greenlee, M. W. (2000). Attentional suppression of activity in the human visual cortex. *Journal of Vision*, (2), 271–277.
- Tanaka, Y., Miyauchi, S., Misaki, M., & Tashiro, T. (2007). Mirror symmetrical transfer of perceptual learning by prism adaptation. *Journal of Vision*, (10), 1350–1361.
- Treue, S. (2001). Neural correlates of attention in primate visual cortex. *Journal of Vision*, (5), 295–300.
- Wang, R., Zhang, J. Y., Klein, S. A., Levi, D. M., & Yu, C. (2012). Task relevancy and demand modulate double-training enabled transfer of perceptual learning. *Journal of Vision*, (12), 33–38.
- Xiao, L. Q., Zhang, J. Y., Wang, R., Klein, S. A., Levi, D. M., & Yu, C. (2008). Complete transfer of perceptual learning across retinal locations enabled by double training. *Journal of Vision*, (24), 1922–1926.
- Zhang, J. Y., Zhang, G. L., Xiao, L. Q., Klein, S. A., Levi, D. M., & Yu, C. (2010). Rule-based learning explains visual perceptual learning and its specificity and transfer. *Journal of Vision*, (37), 12323–12328.
- Zhang, T., Xiao, L. Q., Klein, S. A., Levi, D. M., & Yu, C. (2010). Decoupling location specificity from perceptual learning of orientation discrimination. *Journal of Vision*, (4), 368–374.